

Image Registration based on Edge Dominant Corners

Rabih Al Nachar¹, Elie Inaty¹, Patrick J Bonnin² and Yasser Alayli²

¹Department of Computer Engineering, University of Balamand, PO Box 100, Elkoura, Lebanon

²Laboratoire d'Ingénierie des Systèmes de Versailles-LISV, 10-12 Av de l'Europe, 78140 Vélizy, France

Keywords: Image Edges, Dominant Corners, Affine Transformation, Polygonal Approximation, Primitive.

Abstract: This paper presents a new algorithm for image registration working on an image sequence using dominant corners located on the image's edges under the assumption that the deformation between the successive images can be modeled by an affine transformation. To guarantee this assumption, the time interval between acquired images should be small like the time interval in a video sequence. In the edge image, dominant corners are extracted per linked contour and form a polygon that best approximates the current linked contour. The number of these dominant corners per contour is derived automatically given an approximation error. These dominant corners are shown to be very repeatable under affinity transformation. Then, a Primitive is constructed by four dominant corners. The invariant measure that characterizes each primitive is the ratio of areas of two triangles constructed by two triplets selected from these four corners.

1 INTRODUCTION

Image registration (Zitova and Flusser, 2003) is the process that determines the geometric model or transformation that aligns the points in two images of the same scene taken at different viewpoints, different times, or even different camera types.

It is used in different fields like image matching (Almehio and Bouchafa, 2010), stereovision (Gouiffes, Lertchuwongsa and Zavidovique, 2011), image mosaicking and animation (Wong, Kovesi and Datta, 2007 and Zhi-guo, Ming-Jia and Yu-qing, 2012), motion analysis (Bouchafa and Zavidovique, 2006) and especially medical imaging (Maurer and Fitzpatrick, 1993). The new image registration algorithm presented in this paper is targeting mainly motion analysis where the deformation between the source image and the target one can be modeled by an affine transformation.

In recent years, many approaches have been developed in this area, leading to a great evolution of registration techniques (Zitova and Flusser, 2003). Those techniques can be classified in general as spatial or frequency domain techniques. Spatial methods rely directly on image intensities or image features like edges (Wenchang, Jianshe, Xiaofei and

Lin, 2010 and Zhi-guo, Ming-Jia and Yu-qing, 2012), contours (Kumar, Arya, Rishiwal, and Joglekar, 2006 and Li, Manjunath and Mitra, 1995), regions (Chum and Matas, 2006), interest points (Lin, Du, Zhao, Zhang and Sun, 2010) and lines (Almahio and Bouchafa, 2010). While frequency methods apply phase correlation between the pair of images to extract the transformation model (Wolberg and Zokai, 2000).

An application for the presented algorithm is also camera stabilization in video mode for smoothing the movement by reducing the effect of camera in motion. The video images acquired have a small time interval between them so the deformation can be well modeled by an affine transformation.

This paper is organized as follows: Section 2, explains how an existing polygonal approximation algorithm extracts dominant corners. In Section 3 we describe the first proposed process which is the automatic selection of these corners. We present the primitive construction procedure and its invariant measure and explain the concept of voting scheme in section 4. Section 5 shows some experimental results on synthetic and real images. Finally, a conclusion presents a summary of the work.

2 AN OVERVIEW ON POLYGONAL APPROXIMATION AND DOMINANT CORNERS

Edges are one of the most important features in the image domain that have great immunity against contrast variation. On these edges, corners (Nachar, Inaty, Bonnin and Alayli, 2012 and 2013), which are the intersections of non collinear straight edges, are extracted. Among these corners dominant corners (DCs) are selected. These DCs construct the vertices of the polygon approximating a linked edge or contour. Next, we will summarize the process of corners elimination to have only DCs. More details can be found in (Nachar, Inaty, Bonnin and Alayli, 2013)

2.1 Integral Square Error of a Segment

Each segment joining two corners is characterized by a measure called Integral Square Error (ISE) between the portion of the edge limited by those two corners and the segment itself (Carmona-Poyato, Madrid-Cuevas, Medina Carnicer and Munoz-Salinas, 2010).

2.2 Iterative Elimination of Corners

The process of corners elimination is an iterative process. Initially, each corner C is represented by the ISE of the segment joining its two direct neighbors [CpCn] as described in Figure 1. The term Global ISE denoted by GISE is the sum of all segments ISEs.

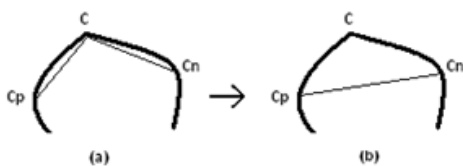


Figure 1: Corner Elimination.

Consider the edge part shown in Figure 1. Figure 1 (a) show an edge part in bold, three corners and the two segments of a polygon joining them. Figure 1 (b) shows the resulting segment [CpCn] due to the removal of corner C. The elimination of a corner is based on a measure called "Cost of Removal" denoted by CR which is the error induced

to the GISE if the current corner is removed. Mathematically, if C is the current corner, its CR is

$$CR_C = ISE_{[CpCn]} - (ISE_{[CpC]} + ISE_{[CCn]}) \quad (1)$$

CR_C represent the area of the triangle $CpCn$. Iteratively, the corner C with the smallest CR is removed first, its CR is added to GISE and the CR of the direct neighbors is updated since Cn becomes a direct neighbor for Cp instead of C and vice versa.

Finally, these non eliminated corners are the DCs and form the vertices of the polygon approximating the edge (Nachar, Inaty, Bonnin and Alayli, 2013).

3 PROPOSITION ONE: AUTOMATIC SELECTION OF DOMINANT CORNERS AND STOPPING CRITERION

The basic feature that should be added to the algorithm presented in (Nachar, Inaty, Bonnin and Alayli, 2013) in order to be used in an application like image registration is the automatic selection of dominant corners. The goal is to select only the corresponding DCs on every couple of corresponding contours in both images. Assume that two images are taken of the same scene but at different viewpoints, non corresponding edges could appear. Even corresponding edges in the two images may have different number of corners. Therefore, we cannot rely on a compression factor as a stopping criterion because it will lead to a lot of non corresponding corners. On the other hand, even corresponding corners may have different ISE values if the scaling factor relating the two images is relatively high.

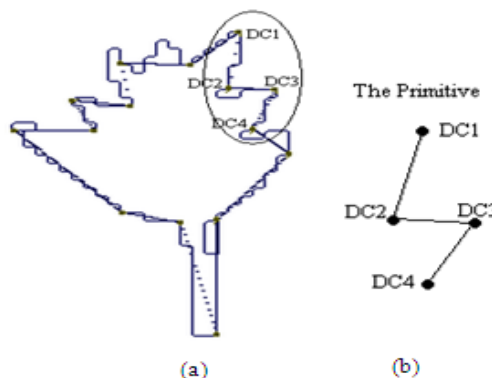


Figure 2: Grouping four consecutive DCs into one primitive.

As mentioned in Section 2, the basic measure according to it a corner could be removed is the CR that will be added iteratively to the GISE. From one side, this GISE is equal to the sum of ISEs of segments constructed by non eliminated corners where each ISE is equivalent to the area limited by the corresponding segment and edge part. So, GISE is a sum of areas which is an area. On the other hand, the affine transformation has the ratio of areas an invariant parameter (Hartley and Zisserman, 2003). So taking the ratio of the current GISE with respect to the initial one is a good measure that can be used as a stopping criterion. While eliminating the corners one after the other, GISE will increase. Thus, we can stop the elimination automatically by setting a fixed threshold r . This way, even when the scaling parameter between the two images is considerable, we can still obtain only corresponding DCs in both images.

Affine transformation has the ratio of areas as an invariant parameter, thus the ratio of CRs is preserved under affine transformation. Therefore, we can state that any two CRs ($CR1 > CR2$) corresponding to two corners on the same contour, will remain in the same order under an affine transformation. So, the order of CRs is invariant with respect to an affine transformation. Therefore, we expect that only corresponding DCs will show up in an image and the transformed one since the elimination of a corner is based on its CR value compared to others CRs.

4 PROPOSITION TWO: GROUPING DCS INTO PRIMITIVES AND VOTING SCHEME:

4.1 Primitive Construction

Based on high reoccurrence of DCs, a primitive is formed by grouping four consecutive DCs. The average of the four corners ISEs is set as the primitive ISE. Here, primitives are classified according to their ISE. The strongest primitives are those who have the highest ISEs. The vote of each primitive will be biased by its ISE since strong primitives are formed by DCs of high ISEs. This means that the corners are of high repeatability or high probability of occurrence in both images.

In Figure 2, a polygon of fifteen DCs as vertices approximating the contour of a leaf image is shown. The four circled DCs are grouped into one

primitive. Two triangles $DC1\widehat{DC2}DC3$ and $DC2\widehat{DC3}DC4$ are considered. The ratio of their area R will be used for matching with other primitives in the second transformed image.

Consider now two images related by an affinity. The primitives are formed in both images and each primitive is characterized by its two parameters R and ISE. We adopt a group voting scheme based on Hough transform (Zhongke, Xiaohui and Lenan, 2003) for the six unknown parameters of the affine transformation. The idea behind the Hough transform is to accumulate, in a space of representative parameters, the information that assures the presence of a certain shape or model. In our case, the desired model to find is an affine model that has six unknowns. So, our Hough space has six parameters and each matched couple of primitives from the two images will increase by one the accumulator of the corresponding point in this space. Three points are enough to calculate these parameters. Each primitive will vote for a set of six parameters and the set that gets the highest votes will be selected. Let $DC_1(x_1, y_1)$, $DC_2(x_2, y_2)$, $DC_3(x_3, y_3)$ and $DC_4(x_4, y_4)$ be the DCs constructing a primitive in the first image and $DC'_1(x'_1, y'_1)$, $DC'_2(x'_2, y'_2)$, $DC'_3(x'_3, y'_3)$ and $DC'_4(x'_4, y'_4)$ be the DCs constructing the corresponding primitive in the second image. The affine transformation presented in (1) can be rewritten as,

$$\begin{pmatrix} x'_1 \\ x'_2 \\ x'_3 \end{pmatrix} = \begin{bmatrix} x_1 & y_1 & 1 \\ x_2 & y_2 & 1 \\ x_3 & y_3 & 1 \end{bmatrix} \begin{pmatrix} a_{11} \\ a_{12} \\ tx \end{pmatrix} \text{ or } X' = M \cdot h \quad (2)$$

$$\begin{pmatrix} y'_1 \\ y'_2 \\ y'_3 \end{pmatrix} = \begin{bmatrix} x_1 & y_1 & 1 \\ x_2 & y_2 & 1 \\ x_3 & y_3 & 1 \end{bmatrix} \begin{pmatrix} a_{21} \\ a_{22} \\ ty \end{pmatrix} \text{ or } Y' = M \cdot h' \quad (3)$$

The affine parameters presented in vectors h and h' are calculated in (4) and (5), respectively:

$$h = M^{-1} \cdot X' \quad (4)$$

$$h' = M^{-1} \cdot Y' \quad (5)$$

4.2 Corresponding Primitives Refining

Using only the ratio R to match two primitives will lead to a lot of false positive matches. This means that two non corresponding primitives that have similar ratio of areas are considered by the algorithm as corresponding. To minimize or even eliminate these false positives, we propose to use the corners directions. These directions are the directions of the two meeting straight edges coded in Freeman code (0,4 for horizontal right-left, 2,6 for vertical up-down, 1,5 for first diagonal and 3,7

for second diagonal (Freeman and Davis 1977)). We show experimentally that the detected corners are very repeatable against affine transformation. Also they conserve their angle directions.

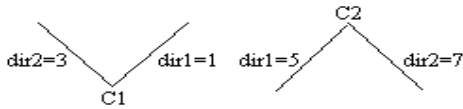


Figure 3: Two corresponding corners.

Figure 3 shows two corresponding corners C1 and C2 rotated by 180° one with respect to the other. It is clear that the difference between dir1 of both corners is equal to that between dir2. This difference reflects the amount of rotation between the two corners. Our proposition for correspondence and voting is stated as follows:

- For every couple of primitives P_1 and P_2 having similar ratio R .
- If the difference between the directions of the four corresponding corners in both primitives is the same:
 - ✓ Form four triplets of three points in each primitive. For example in P_1 : $S_1 =$

$$\{DC_1, DC_2, DC_3\}, S_2 = \{DC_1, DC_2, DC_4\}, S_3 = \{DC_1, DC_3, DC_4\}, S_4 = \{DC_2, DC_3, DC_4\}.$$

- ✓ Use the four sets in P_1 with those corresponding sets in P_2 to calculate four affine models.
- ✓ Calculate the mean model AM_m .
- ✓ If the difference between the models is relatively small, we report that P_1 and P_2 are corresponding and at the same time they give their vote for AM_m .
- Else, select a new couple of primitives.

Using this method, we involve the four points in the parameters calculation. Here if two primitives are really corresponding, the included corners should have same directions difference and also the four formed models should be very close. When the number of votes is not relatively high, we can form an additional set of primitives and thus an additional number of voters. In this set, a corner is grouped with its three nearest neighboring DCs to form a primitive. This way of grouping is also invariant under various transformations. The overall algorithm is fully presented in Figure 4.

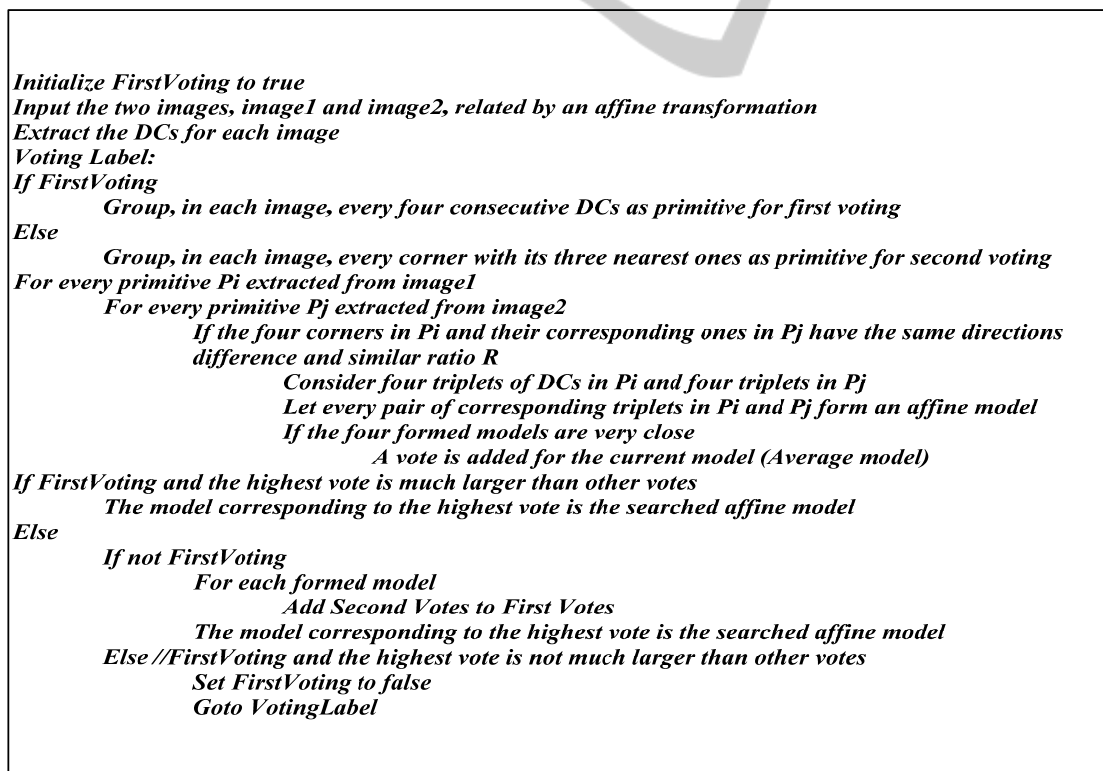


Figure 4: Proposed algorithm.

5 EXPERIMENTAL RESULTS

The experimental results are shown using synthetic and real images. First, a source synthetic image is used and the target image is generated using a well known affine transformation. Thus, the six affine parameters are known a priori. The first results will show the accuracy of the algorithm by showing the relative error between the generated affine model by our algorithm and the given one. The second part will show the repeatability of DCs under various deformations between the source and target images caused by affine transformation. In the third part, synthetic images presented in (Almehio, 2012) are used to compare their results with ours. Given the affine model, the mapping between DCs in the source image and those in the target is known and it is used to show their repeatability.

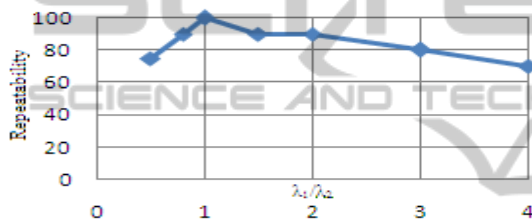


Figure 6: Repeatability of DCs versus scaling factor λ_1/λ_2 ($\theta = 10^\circ$, $\varphi = 15^\circ$ and $\lambda_2 = 1$).

Figure 5 shows a source leaf image and its target generated using an affine model with the following values: $a_{11} = 0.8800$, $a_{12} = 0.1907$, $a_{21} = -0.1008$, $a_{22} = 0.7728$ (corresponding to $\theta = 10^\circ$, $\varphi = 15^\circ$, $\lambda_1 = 1.1$ and $\lambda_2 = 1.3$ presented in section 2), $t_x = -150$, $t_y = 15$. Setting the threshold r (ratio of current GISE and initial GISE used as a stopping criterion as described in section 4) to be $r=5$, the number of DCs extracted in the source image shown in Figure 5 (a) is 16 out of 98 corners while their number in the target image shown in Figure 5 (b) is 17 out of 122 among them 15 DCs are corresponding ones.



Figure 5: Polygonal Approximation and DCs of a source and target leaf images.

In Figure 6, the repeatability of DCs versus the scaling factor λ_1/λ_2 is evaluated. The minimal value of this repeatability is 70% at scale ratio of four which is considered high when dealing with the suggested application of video image sequence with small interval time. Figure 7 shows the repeatability of DCs versus scaling angle φ . It is clear that the worst repeatability is 75% which is also very good and will lead to a high repeatability of the formed primitives. Figure 8 presents the repeatability versus the rotation angle θ between the source and the target images. Also, the worst repeatability is 85% which means that the rotation angle θ has the least influence on the repeatability value. In these results, we have selected the stopping criterion as the remaining number of DCs. It was chosen equal to 20DCs.

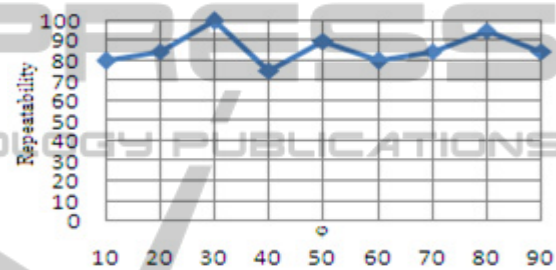


Figure 7: Repeatability of DCs versus scaling angle φ ($\theta = 10^\circ$, $\lambda_1 = 1.3$ and $\lambda_2 = 0.8$).

We can even obtain higher repeatability if we select for example 80% of these DCs that correspond to the highest ISEs. In Figure 7, it is shown that for the given values of the affine parameters ($\varphi = 10^\circ$, $\lambda_1 = 1.3$, $\lambda_2 = 0.8$ and $\theta = 90^\circ$) the repeatability of DCs is 85% (17 corresponding DCs out of 20). If we select only 80% of these DCs, the repeatability becomes 93.75% (15 corresponding DCs out of 16).

Now we will show the relative error between the real affine model relating two synthetic images and the estimated model by our algorithm. These

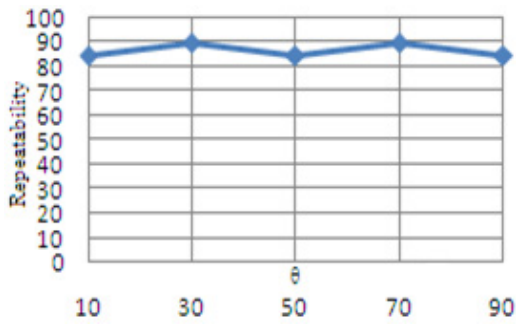


Figure 8: Repeatability of DCs versus rotation angle θ ($\phi = 10^\circ$, $\lambda_1 = 1.3$ and $\lambda_2 = 0.8$).

images (Almehio, 2012) are shown in Figure 8 and the results are reported in Table 1.

Table 1: Estimated affine models.

	a_{11}	a_{12}	a_{21}	a_{22}	t_x	t_y
Real Model M	0.9	0	0.05	0.85	0	0
Our Model M'	0.91	-0.04	-0.04	0.81	2	4
Model M'' in (Almehio 2012)	0.88	0.008	0.05	0.85	-0.1	-7.7

To compare the results presented in Table 1, the mean square errors MSE_o between our model and

the real one and MSE_A between Almehio model and the real one are derived in (6) and (7).

$$MSE_o = \frac{1}{6} \sum_{i=0}^5 (H'_i - H_i)^2 = 3.335 \quad (6)$$

$$MSE_A = \frac{1}{6} \sum_{i=0}^5 (H''_i - H_i)^2 = 9.883 \quad (7)$$

Figure 10 shows two real images taken from a video sequence in (Almehio and Bouchafa, 2010). Two matched primitives are shown in Figure 9 and the image of difference between the source and target images is revealed in Figure 11. In this image, each pixel's intensity is obtained by taking the absolute difference of corresponding pixels intensities in both images. Thus darker pixels represent higher difference between the compared intensities in both images. Also, the alignment between the two images is shown in Figure 11. Let us concentrate on the arrow shape circled in both images source and target of Figure 11. We see, in Figure 12, that part of this shape is dark and part is bright. The dark part correspond to a big difference between the two arrow shapes in the source and target images and that is normal due to the difference in the 3D position of the two shapes. Thus, aligning these two shapes will make the intersection part bright and the other part dark in the image of difference. The same discussion can be made on every corresponding part in both images.

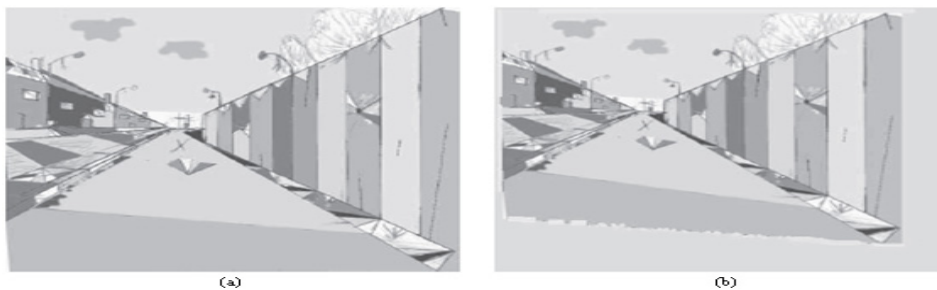


Figure 9: Synthetic images (Almehio, 2012). (a) Source image. (b) Target image.



Figure 10: Two tested real images of a common scene (Almehio and Bouchafa, 2010).

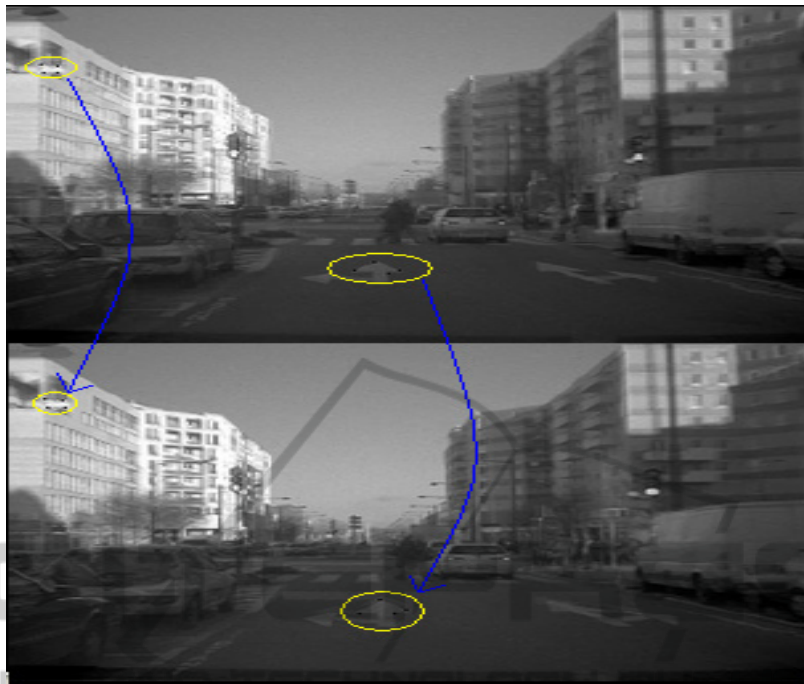


Figure 11: Two matched primitives circled in yellow in the two real images.



Figure 12: Image of Difference between source and target images.

In real images, the number of corresponding DCs, thus the number of matched primitives, is less than those in synthetic images due to the complexity of these real images. Also, the numbers of false positive and true negative matches increase using real images. However, using group primitive voting or the sum of all votes leads in most cases to the true model with a good difference with the nearest false one.

6 CONCLUSIONS AND FUTURE WORK

In this paper, a novel technique for image registration using dominant corners located on image edge is presented. First, corners are detected using an edge plus corner detector than only corners that form the vertices of the polygon that best approximates every image contour are considered and called "Dominant corners". It was shown experimentally that these DCs have very good repeatability versus affine transformation. Primitives are then formed by grouping every four

corners: consecutive and nearest. The ratio of two triangles in every primitive construct the invariant measure used to match a couple of primitives in a source and target images. The voting scheme uses three test for matching: matching the four corners directions, the matching of the votes of the four triplets selected in one primitive and the matching of the primitive area ratio R . This scheme eliminates a lot of false matching and makes the difference high between the number of votes for the correct model and other false ones.

The suggested algorithm can be used in image registration and especially in motion analysis application when the time interval between sequences of images is relatively small.

REFERENCES

- Almeio Y. and Bouchafa S., 2010. *Matching image using invariant level-line primitives under projective transformation*. In *Canadian Conference on Computer and Robot Vision (CRV)*.
- Gouiffes N., Lertchuwongsa N. and Zavidovique B., 2011. *Mixed color/level lines and their stereo-matching with a modified hausdorff distance*. Integrated Computer-Aided Engineering.
- Wong T., Kovesi P. and Datta A., 2007. *Projective Transformations for Image Transition Animations*. 14th International Conference on Image Analysis and Processing (ICIAP).
- Bouchafa S. and Zavidovique B., 2006. *Efficient cumulative matching for image Registration*, Image and Vision Computing, 24.
- Maurer C.R. and Fitzpatrick J. M., 1993. *A review of medical image registration*, in *Interactive Image-Guided Neurosurgery (R. J. Maciunas, ed.)*, pp. 17–44, Park Ridge, IL: American Association of Neurological Surgeons.
- Wenhang S., Jianshe S., Xiaofei G. and Lin Z., 2010. *An improved InSAR image registration algorithm*, 2nd International Conference on Industrial Mechatronics and Automation (ICIMA), vol 2.
- Lin H., Du P., Zhao W., Zhang L. and Sun H., 2010. *Image registration based on corner detection and affine transformation*, 3rd International Congress on Image and Signal Processing, vol 5.
- Zhi-guo W., Ming-Jia W. and Yu-qing W., 2012. *Image Mosaic Technique Based on the Information of Edge*, 3rd International Conference on Digital Manufacturing and Automation (ICDMA).
- Chum O. and Matas J., 2006. *Geometric Hashing with Local Affine Frames*, IEEE Computer Society Conference on Computer Vision and Pattern Recognition, vol 1.
- Li H., Manjunath S. and Mitra S.K., 1995. *A Contour-Based Approach to Multisensor Image Registration*, IEEE Transactions on Image Processing, vol 4.
- Zitova B. and Flusser J., 2003. *Image registration methods: a survey*, Image and Vision Computing 21.
- Wolberg G. and Zokai S., 2000. *Robust image registration using log-polar transform*, Proceedings of IEEE International Conference on Image Processing, vol 1.
- Nachar R., Inaty E., Bonnin P. and Alayli Y., 2012. *A Robust Edge Based Corner Detector*, Submitted for possible publication in Autonomous Robots Springer, September 2013, August 2013, under review.
- Nachar R., Inaty E., Bonnin P. and Alayli Y., 2013. *Polygonal Approximation of an Object Contour by Detecting Edge Dominant Corners Using Iterative Corner Suppression*, Submitted for possible publication in Autonomous Robots Springer, September 2013, August 2013, under review.
- Hartley R. and Zisserman A., 2003. *Multiple View Geometry in Computer Vision*, Cambridge university press, 2nd Edition.
- Zhongke L., Xiaohui Y. and Lenan W., 2003. *Image registration based on hough transform and phase correlation*, Proceedings of the 2003 International Conference on Neural Networks and Signal Processing, vol 2.
- Carmona-Poyato A., Madrid-Cuevas F.I., Medina Carnicer R. and Munoz-Salinas R., 2010. *Polygonal approximation of digital planar curves through break point suppression*, Pattern Recognition, 43(1), pp. 14-25.
- Kumar S., Arya K.V, Rishiwal V. and Joglekar P.N., 2006. *Robust Image Registration Technique for SAR Images*, First International Conference on Industrial and Information Systems.
- Freeman H. and Davis L.S., *In A Corner Finding Algorithm for Chain Coded Curves*. IEEE Transaction in Computing, Vol. 26. 1977.
- Almeio Y., 2012. *A Cumulative Framework for Image Registration using level-line Primitives*, PhD thesis, Universite Paris Sud XI.